PNAS RESEARCH ARTICLE | IMMUNOLOGY AND INFLAMMATION

A TGF-βR/IL-2R immunomodulatory fusion protein transforms immunosuppression into T cell activation to enhance adoptive T cell therapy

Yapeng Su[a,b,1], Ashley Thelen[a,1,2], Lena V. Wirth[a], Cody M. Jenkins[a], Sam R. Mak[a], Daniel G. Chen[a,c,d], Raphael Gottardo[e], and Philip D. Greenberg[a,f,g,2]

Affiliations are included on p. 9.

Contributed by Philip D. Greenberg; received July 3, 2025; accepted August 18, 2025; reviewed by James P. Allison and Robert D. Schreiber

Adoptive T cell therapies have shown limited efficacy against solid tumors due in part to immunosuppressive cues such as from TGF-β and insufficient survival/proliferative signals within the tumor microenvironment (TME). We engineered chimeric immunomodulatory fusion proteins (IFPs) that convert immunosuppressive TGF-β signals into proliferative/survival Interleukin 2 (IL-2) signals in T cells. Chimeric TGF-βR/IL-2R IFPs were constructed by fusing extracellular domains of the TGF-β receptor chains with intracellular domains of IL-2Rβ and IL-2Rγ to enable TGF-β binding to trigger STAT5 phosphorylation and activate the downstream IL-2 pathway. In human primary CD8$^+$ T cells, select IFP designs robustly induced p-STAT5 upon exposure to TGF-β1, and simultaneously reduced canonical SMAD2/3 signaling. IFP-expressing T cells proliferated and displayed enhanced viability in response to TGF-β1, effectively leveraging TGF-β-rich conditions to outcompete nontransduced cells. Transcriptomic analyses revealed that IFP signaling promoted T cell activation and allowed maintenance of stemness during culture with TGF-β. Functionally, coexpressing IFPs with a mesothelin-specific T cell receptor improved tumor killing and promoted T cell expansion in the presence of TGF-β1, highlighting both neutralization of TGF-β–mediated suppression and enhanced proliferation. TGF-βR/IL-2R IFPs appear promising for reprogramming the signals T cells receive in the TME and improving efficacy of adoptive T cell therapy in solid tumors.

cancer immunotherapy | adoptive T cell therapy | T cell engineering | T cell receptor (TCR) T cell therapy

Significance

Adoptive T cell therapy has shown limited success in solid tumors due in part to immunosuppressive factors such as Transforming growth factor (TGF)-β and to limited proliferative signals within the tumor microenvironment. We developed a class of immunomodulatory fusion proteins (IFPs) that rewire suppressive TGF-β signals into proliferative/survival Interleukin 2 (IL-2) signals, enhancing T cell function, persistence, and tumor cell killing. These engineered synthetic TGF-βR/IL-2R IFPs simultaneously neutralize TGF-β-mediated inhibition and promote IL-2 pathway activation, offering a strategy to improve T cell performance in the hostile tumor environment. Our findings provide a framework for designing synthetic receptors that can sustain T cell activity and should help advance a next generation of increasingly effective cellular therapies for solid tumors.

Adoptive T cell therapies with engineered T cells have achieved remarkable success in hematologic malignancies (1), but face persistent challenges in solid tumors due in part to hostile tumor microenvironments (TME) dominated by immunosuppressive factors and a scarcity of prosurvival/proliferative cytokine signals such as from Interleukin 2 (IL-2) (2, 3). TME suppression of infiltrating CD8$^+$ T cells is mediated through multiple mechanisms including TGF-β–mediated suppression of effector functions and limited access to IL-2, a cytokine critical for T cell survival and proliferation, particularly for T cell receptor (TCR)-engineered CD8$^+$ T cells which lack the "built-in" costimulatory signals present in CAR-T cell constructs (4, 5). TGF-β directly attenuates CD8$^+$ T cell cytotoxicity in part by downregulating the transcription factor T-bet (6), while simultaneously promoting differentiation of endogenous CD4$^+$ T cells within the TME toward an immunosuppressive regulatory T cell (Treg) phenotype (5). Concurrently, the effects of insufficient IL-2 within the TME are exacerbated by elevated levels of TGF-β, which further downregulate IL-2 production and signaling in T cells, impairing sustained activation and expansion of antitumor T cells and undermining effector functions and memory responses (4).

Approaches to circumvent TME-mediated immunosuppression have often been limited by off-tumor toxicity due to lack of selectivity at the tumor site, as with systemic TGF-β neutralization or high-dose IL-2 administration. Systemic TGF-β blockade risks toxicity to normal tissues such as cardiac function/injury (7), reflecting the cytokine's pleiotropic and beneficial roles in tissue homeostasis (8). Similarly, systemic delivery of exogenous IL-2 is not selective for the infused target cells, and can both expand immunosuppressive Treg cells and induce morbidity from toxicities such as capillary leak syndrome (9). A dominant-negative TGF-β receptor II (dnTGF-βRII) has been explored as a strategy to sequester TGF-β ligands without triggering downstream signaling- however, the dnTGF-βRII alone failed to sustain CAR-T cell expansion or persistence, as it does not provide adequate proliferative or prosurvival signals to the engineered T cells (10). Such

Reviewers: J.P.A., MD Anderson; and R.D.S., Washington University in St. Louis School of Medicine.

Competing interest statement: A.T. is currently employed by Juno Therapeutics/Bristol-Myers Squibb. R.G. has received consulting income from Takeda, Sanofi, Arcellx, Owkin, and declares ownership in Ozette Technologies. P.D.G. has stock in Affini-T Therapeutics, Elpiscience, Immunoscape, Earli, Rapt, Catalio, and Nextech. A.T. and P.D.G. have a pending patent application related to this work filed. Co-author P.D.G. and reviewer R.D.S. have co-authored multiple non-research mission statements for AACR journals.

[1]Y.S. and A.T. contributed equally to this work.

[2]To whom correspondence may be addressed. Email: thelen.ashley.m@gmail.com or pgreen@uw.edu.

This article contains supporting information online at https://www.pnas.org/lookup/suppl/doi:10.1073/pnas.2516951122/-/DCSupplemental.

Published September 23, 2025.

prosurvival and proliferative signals can be crucial for therapeutic benefit by TCR-engineered T cells in solid tumors which require a persistent response (11).

In response to these and related obstacles, emerging approaches have explored synthetic fusion proteins that can be used to reprogram immune signals selectively in only the engineered transferred T cells (12), which, because they specifically recognize tumor cells, will be enriched and activated mainly in the TME. This approach has the potential to avoid systemic toxicity while addressing impediments such as immunosuppressive factors that impact survival and function of T cells in the TME. For example, a Fas-4-1BB IFP that fuses the extracellular domain of Fas to the intracellular domain of 4-1BB converts FasL-induced apoptosis into prosurvival and proliferative signals via NF-κB and PI3K pathways, and has been demonstrated to enhance antitumor activity in pancreatic and leukemia models (13). A CD200R-CD28 IFP that redirects the inhibitory signal from CD200R into CD28 costimulation can promote T cell proliferation and has been shown to improve leukemia clearance while bypassing dependency on exogenous IL-2 (14). Similarly, a PD-1-CD28 IFP that replaces the immunosuppressive tail of PD-1 with the CD28 cytoplasmic tail can rescue T cells from PD-L1–mediated exhaustion (15).

Building on these strategies, we have evaluated TGF-βR/IL-2R immunomodulatory fusion proteins (IFP) with the goal of converting immunosuppressive TGF-β signals into IL-2-mediated activation signals. By simultaneously neutralizing a key immunosuppressive signal and delivering prosurvival and proliferative cues, this strategy has the potential to reprogram TME signals to enhance rather than diminish the efficacy of adoptive T cell therapy in solid tumors.

Results

Design of TGF-βR/IL-2R IFPs to Convert TGF-β1 Signaling into an IL-2 Signal to Enhance T Cell Function. We engineered IFPs to repurpose TGF-β1 stimulation for delivery of IL-2 activation signals via inducing STAT5 phosphorylation (p-STAT5) (Fig. 1*A*). TGF-βR/IL-2R IFPs were constructed by fusing the extracellular ligand-binding domains of TGF-βRI and TGF-βRII with the intracellular signaling domains of IL-2Rβ and IL-2Rγ, as a strategy to enable TGF-β1 to engage and trigger the IL-2 receptor signaling cascade. Given the structural complexity of the TGF-β and IL-2 receptor families, with the former signaling as a 4 chain heterodimer of 2 homodimers and the latter being a 3 chain heterotrimer that contains 2 signaling cytoplasmic tails (16–18), we generated four distinct IFP constructs with varied pairings of domains and transmembrane regions to determine whether the specific structure and orientation impacts ligand binding, signal transduction, assembly, and/or competition with endogenous chains (Fig. 1*B*). Each construct was designed with bicistronic expression elements that incorporate all the required receptor chain components with a furin cleavage site inserted after the first chain and before a P2A self-cleaving peptide sequence to ensure efficient expression and proper posttranslational processing, and to remove the extraneous P2A sequences from the expressed protein. By fusing the IL-2Rβ and IL-2Rγ cytoplasmic domains to distinct ligand binding TGF-βRI and TGF-βRII extracellular domains, we ensured that each tetrameric signaling complex contained both IL-2 signaling modules. The resulting four-chain complex should have higher affinity for TGF-β1 compared to fusing IL-2R chains to only dimeric TGF-βRII or dimeric TGF-βRI and also mitigates the risk of excessive IL-2 signaling, which can lead to activation-induced cell death, because the tetrameric complex gets endocytosed and degraded, whereas dimeric forms tend to recycle to the cell surface for continuous signaling (19).

To evaluate the function of these different IFP designs, primary human $CD8^+$ T cells were activated, transduced with the IFP constructs, and exposed to increasing concentrations of recombinant TGF-β1. IL-2R pathway activation was assessed by measuring with flow cytometry levels of phospho-STAT5 (p-STAT5), the downstream IL-2R messenger phosphorylated in response to dimerization of the IL-2Rβ and IL-2Rγ chains (20). Despite comparable transduction efficiency, as measured by expression of the included transduction marker NGFR (*SI Appendix*, Fig. S1*C*), two of the four IFP constructs, the TGF-βRI ectodomain fused to the IL-2Rβ cytoplasmic tail plus the TGF-βRII ectodomain fused to the IL-2Rγ cytoplasmic tail, denoted 1β2γ and with the IL-2 transmembrane (TM) domains, and the TGF-βRII ectodomain fused to the IL-2Rβ cytoplasmic tail plus the TGF-βRI ectodomain fused to the IL-2Rγ chain, denoted 2β1γ and with the TGF-βR TM domains, demonstrated the highest increase in p-STAT5 levels following TGF-β1 exposure, indicating more effective conversion of TGF-β1 binding into a pro-proliferative IL-2 signal (Fig. 1*C*). These two constructs were thus selected as our focus in subsequent analyses. The observed responses were consistent across multiple donor-derived T cell populations, demonstrating reproducibility and efficacy of these IFP constructs (Fig. 1*C*).

To test whether TGF-β binding to the native TGF-β receptor was limiting p-STAT5 activation or function, we used CRISPR-Cas9 to knock out (KO) TGF-βRII in primary human $CD8^+$ T cells. TGF-βRII forms a homodimer that binds dimeric TGF-β1 and delivers it to TGF-βRI, which alone has low affinity for TGF-β1 and cannot form a functional signaling complex without TGF-βRII (16). Successful knockout of TGF-βRII was validated by flow cytometry, showing a complete loss of TGF-βRII surface expression (Fig. 1*D*). TGF-βRII–deficient cells expressing the IFP exhibited STAT5 phosphorylation following TGF-β1stimulation similar to cells lacking the TGF-βRII-knockout, suggesting the engineered IFP receptors effectively signal even in the presence of physiologic TGF-βRII expression (Fig. 1 *C* and *E* and *SI Appendix*, Fig. S1).

Analysis of signaling through the natural TGFβR revealed that stimulation with 0.5 ng/mL of recombinant TGF-β1 induced minimal signaling in wild type or transduced primary $CD8^+$ T cells, whereas 10 or 50 ng/mL of TGF-β1 increased pSMAD2/3 levels in untransduced wild type cells but remained near baseline in cells transduced with the IFP (*SI Appendix*, Fig. S2), consistent with the IFP leading to diminution of canonical TGF-βR signaling. The background detection of pSMAD2/3 in the absence of exogenous TGF-β1 even in TGF-βR–KO cells suggested either a persistent low level of phosphorylation, perhaps via nemo-like kinase (21), or promiscuous binding by the antibody reagent. The reduction in pSMAD2/3 levels in T cells expressing the IFP (*SI Appendix*, Fig. S2) demonstrated that engineered IFP receptors competitively inhibit endogenous TGF-βR signaling by functioning similar to dominant-negative TGFβR chains and/or binding and sequestering the TGF-β1 ligand (22). These results collectively demonstrate TGF-βR/IL-2R IFPs not only rewire TGF-β signaling to promote phosphorylation of STAT5 in T cells, but should also mitigate suppressive effects of endogenous TGF-β signaling mediated via pSMAD2/3.

TGF-β1 Mediates Expansion of $CD8^+$ T Cells Expressing the IFP and Can Select for Transgene-Expressing Cells. Given that the TGF-βR/IL-2R IFPs convert TGF-β1 signals into IL-2-p-STAT5 signals whereas wild-type TGF-βR blocks proliferation (23), we hypothesized the IFPs should also promote selective expansion of

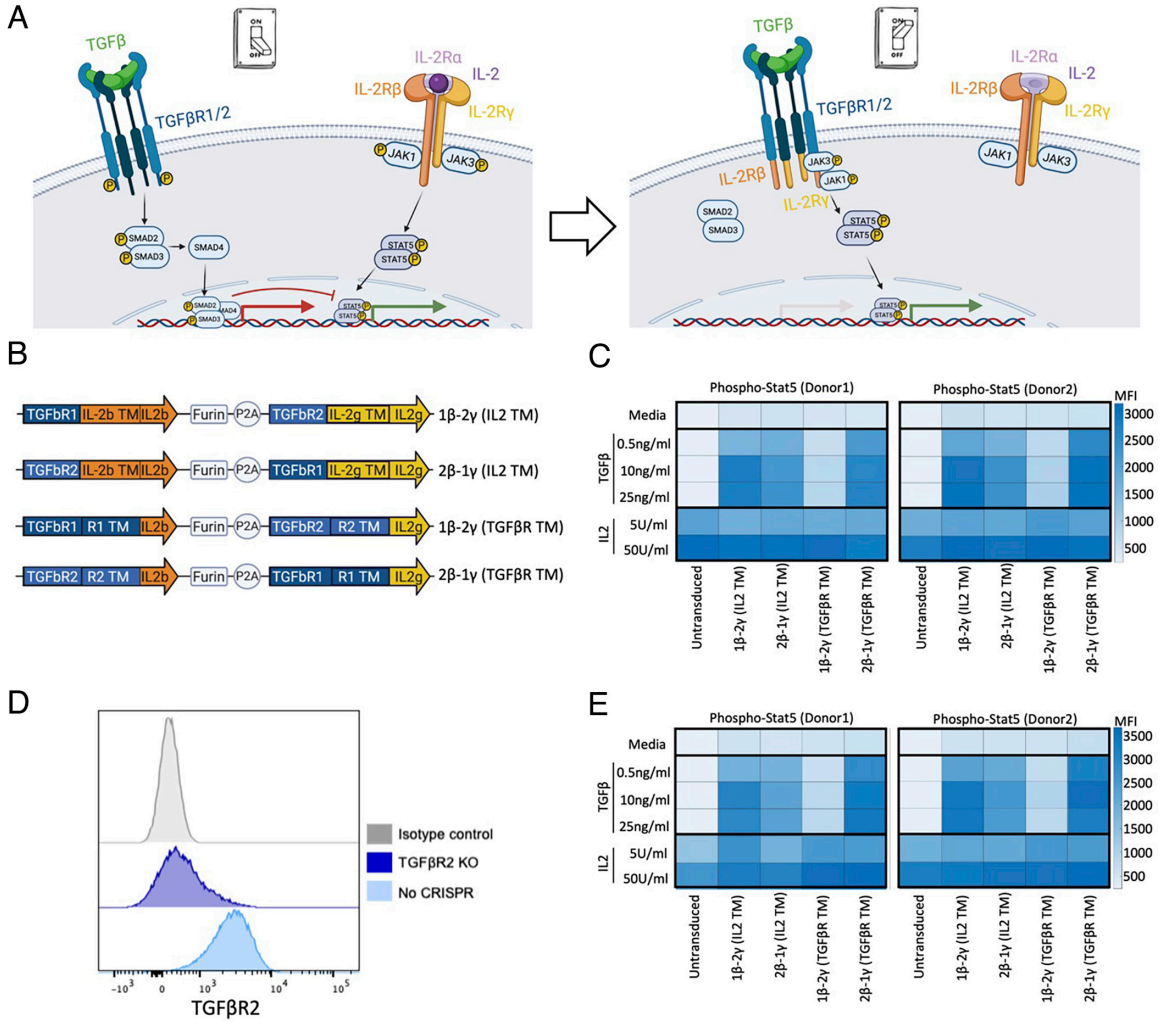

Fig. 1. TGF-βR/IL-2R IFPs repurpose TGF-β to transmit an IL-2 signal via p-STAT5. (*A*) Schematic of endogenous TGF-β and IL-2 signaling (*Left*) and rewired signaling via TGF-βR/IL-2R IFPs (*Right*). *Left*: Endogenously, TGF-β binds TGF-βRII, forming a 2:2:2 receptor–ligand complex with TGF-βRI, activating SMAD2/3, which bind SMAD4 and translocate to the nucleus to suppress T cell proliferation and function; IL-2 binds its trimeric receptor (α, β, γ), activating JAK1/3 and STAT5, promoting transcription of genes driving T cell proliferation, differentiation, and effector function—activities suppressed by TGF-β. *Right*: Rewiring the TGF-β signaling pathway to an IL-2 signaling pathway via TGF-βR/IL-2R IFPs. (*B*) Summary of TGF-βR/IL-2R IFP constructs. Bicistronic constructs were separated by a furin protease cleavage site to remove the attached distinct 2A sequence tags from the translated protein, a GSG linker, and a P2A self-cleaving peptide sequence. Since the TGF-βR and IL-2R complexes each have 2 unique receptor signaling chains with distinct transmembrane domains, the possible combinations of extracellular, intracellular, and transmembrane domains yielded four distinct construct configurations of IFPs for comparative analyses. (*C*) IFPs convert the TGF-β signal into an IL-2 signal as indicated by increased p-STAT5 upon TGF-β or IL-2 stimulation. Primary CD8 T cells were activated on Day 0, transduced with IFP constructs on Day 1, and cultured for 9 more days in the presence of IL-2, IL-7, and IL-15 to achieve stable transgene expression and then harvested and washed before stimulation with the indicated amounts of recombinant TGF-β or IL-2, followed by fixation/permeabilization and staining with a phospho-specific (Y694) STAT5 antibody. The heatmap shows p-STAT5 levels, quantified as mean fluorescence intensity (MFI) by flow cytometry across different cytokine doses (rows) for T cells engineered with different IFPs (columns). (*D*) Primary human CD8 T cells were electroporated with Cas9 RNP targeting TGF-βRII to knock out the endogenous TGF-βRII as shown by failure to bind an mAb to TGF-βRII relative to the No CRISPR control. (*E*) IFPs convert the TGF-β signal into an IL-2 signal in T cells with the TGF-βR knocked out, as indicated by increased p-STAT5 upon TGF-β or IL-2 stimulation. Primary CD8 T cells were activated, knocked out for TGF-βR, transduced with IFP constructs, cultured for 9 more days in the presence of IL-2, IL-7, and IL-15 as in (*C*), stimulated with the indicated amounts of recombinant TGF-β1 or IL-2, and then fixed/permeabilized and stained with a phospho-specific (Y694) STAT5 antibody. The heatmap shows p-STAT5 levels across different cytokine doses (rows) for T cells engineered with different IFPs (columns).

transduced T cells in the presence of TGF-β1. To investigate the impact of TGF-β1 signaling in cell mixtures containing IFP$^+$ and IFP$^-$ cells, primary human CD8$^+$ T cells, transduced with TGF-βR/IL-2R IFPs in a plasmid backbone that expressed NGFR as a transduction marker were cultured in varying concentrations of recombinant human TGF-β1 or IL-2. There was a significant enrichment over time of transduced cells, as indicated by an increased frequency of NGFR$^+$ cells in cultures supplemented with TGF-β1 compared to IL-2 or media-only conditions (Fig. 2*A*). Notably, following exposure to 25 ng/mL of TGF-β1, nearly 100% of the cells present at day 7 expressed the IFP (Fig. 2*A*), suggesting TGF-β1 can be used to promote positive selection of IFP$^+$ cells and negative selection of IFP$^-$ cells.

To further assess the impact of TGF-β1-mediated signaling on T cell proliferation, primary CD8$^+$ T cells were activated and transduced with the IFP and control constructs and cultured for 4 d in the presence of IL-2, IL-7, and IL-15, washed and labeled with CellTrace Violet (CTV), and stimulated with recombinant TGF-β1 or IL-2 every 48 h. Flow cytometric analysis after 5 d for CTV dilution from proliferation revealed that IL-2 induced dose-dependent proliferation of the T cells regardless of expression of the IFP, whereas TGF-β1 supplementation promoted robust cell division only in IFP-expressing cells (Fig. 2*B*). Notably, TGF-β1 induced proliferation in IFP-expressing cells even at doses as low as 1.25 ng/mL TGF-β1 that was comparable to proliferation driven by 5 U/mL of IL-2 in control cells, further supporting

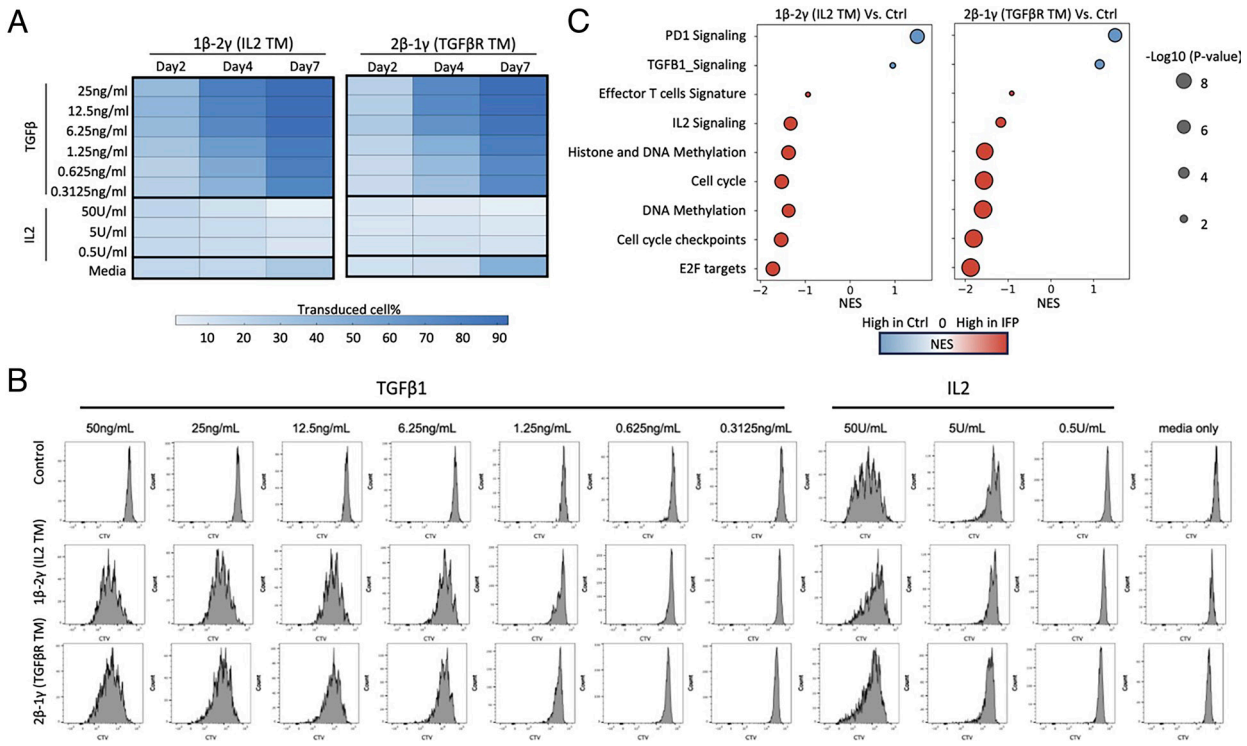

Fig. 2. Culturing human CD8$^+$ T cells expressing the IFP in TGF-β1 drives cell division and selects for transgene expression. (*A*) Transduced T cells cultured in TGF-β1 select for transgene expression. Primary human CD8 T cells were activated with Dynabeads, transduced with [TGF-βRI][IL-2βTM][IL-2β]/[TGF-βRII][IL-2γTM][IL-2γ] denoted as "1β2γ (IL-2 TM)" (*Left*) or [TGF-βRII][TGF-βRIITM][IL-2β]/[TGF-βRI][TGF-βRITM][IL-2γ] denoted as "2β1γ (TGF-βR TM)" (*Right*), and then cultured in the indicated amount of recombinant human TGF-β1 or IL-2 supplemented every 48 h for up to 7 d. % cells expressing the transgenic construct (as measured by staining for the transduction marker NGFR) were tracked. (*B*) TGF-β1 promotes cell division in T cells expressing a TGF-βR/IL-2R IFP. Primary human CD8$^+$ T cells were activated and transduced as above. After 4 d of culture to ensure stable expression of the IFP transgene, cells were washed, labeled with CTV, and cultured for an additional 5 d with recombinant human TGF-β1 or IL-2 at the indicated concentrations with the cytokine replenished every 48 h. Proliferation was assessed by CTV dilution via flow cytometry. (*C*) GSEA for pathways differentially enriched in T cells with each of the IFPs compared to control T cells after culture with TGF-β. T cells were activated on Day 0, transduced on Day 1, and cultured with TGF-β for 10 d. Cells were sorted on Day 10 for live NGFR$^+$ cells for bulk RNA-seq. Dot size represents adjusted *P*-value. Color represents normalized enrichment score (NES). A positive (red) NES means the gene set is upregulated in Ctrl T cells and a negative (blue) NES means the gene set is upregulated in IFP-engineered T cells.

the function of the chimeric receptors in repurposing TGF-β1 signals into a proliferative IL-2–like response.

To gain insight into the transcriptional programs induced by IFP-mediated signaling, we performed gene set enrichment analysis (GSEA) on T cells cultured with TGF-β1 supplementation. The analysis revealed upregulation in IFP-expressing cells compared to control T cells of pathways associated with an effector T cell signature, IL-2 signaling, and proliferation, and decreased TGF-β downstream signaling (Fig. 2*C*). Notably, even in such short-term stimulation conditions, the PD-1 signaling related signatures were already upregulated in control T cells in comparison with IFP engineered T cells (Fig. 2*C*). These findings indicate that TGF-β1 not only supports the survival and expansion of IFP-engineered T cells but also drives transcriptional programs that may enhance functional capacity.

TGF-βR/IL-2R IFPs Enhance Tumor Killing and T Cell Expansion in the Presence of Tumor and TGF-β1. To evaluate the functional impact of TGF-βR/IL-2R IFPs on tumor cell killing, primary human CD8$^+$ T cells transduced to express a mesothelin-specific TCR (TCR_{Msln}), which we have advanced to clinical trials for human pancreatic cancer, either alone or in combination with the IFPs were cocultured for 7 d with PANC-1 tumor cells, which naturally express mesothelin antigen and were genetically labeled with NucLight Red. In the presence of 10 ng/mL of exogenous TGF-β1 added to the cocultures at initiation and then every 48 h, CD8$^+$ T cells expressing the IFP exhibited significantly enhanced tumor elimination compared to T cells expressing only the TCR. This effect was observed at both high (20:1) and more moderate (10:1) effector-to-target ratios, with live-cell imaging showing sustained reduction in live tumor cells over time (as reflected by the reduced area with a NucLight Red signal) in wells containing T cells with an IFP (Fig. 3 *A* and *B*), whereas there was progressive expansion of tumor cells in wells containing T cells lacking the IFP.

In addition to improving tumor killing in IFP-expressing T cells, TGF-β1 also promoted the expansion of T cells expressing the chimeric constructs. Quantification of the fold-expansion of T cells by the final time point (168 h) revealed significantly higher proliferation and survival of T cells expressing both the mesothelin-specific TCR and an IFP compared to those with the TCR alone (Fig. 3*C*). This suggests the engineered IFPs not only sustain functional T cell responses despite the presence of TGF-β1 but also support T cell persistence and expansion in settings modeling components of the immunosuppressive TME, in particular persistent tumor antigen and high TGF-β1 levels. Furthermore, in cocultures supplemented with both TGF-β1 and IL-2, superior tumor clearance and T cell expansion was again observed in IFP-expressing cells across multiple effector-to-target ratios (*SI Appendix*, Fig. S3). Of note, the level of TGF-β1 supplementation in these cocultures is lower than levels reported in the serum of patients with many tumor types (24, 25), and levels in the TME are presumably even higher—such higher levels would be expected to not only suppress endogenous IL-2 production but also further block responsiveness to signaling from the endogenous IL-2R (23, 26). Thus, the IFP, by maintaining both proliferation and tumor cytotoxicity in this immunosuppressive environment, has the

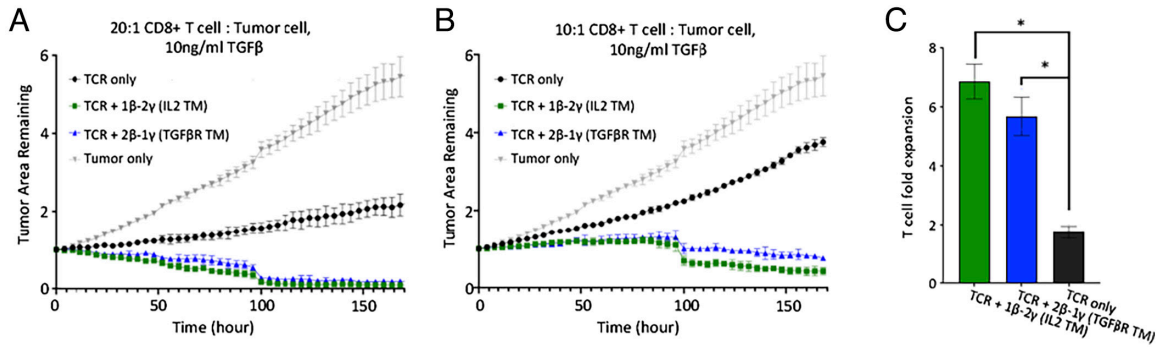

Fig. 3. Cells expressing TCR_{Msln} with a TGF-βR/IL-2R IFP mediate enhanced tumor killing and proliferation in the presence of TGF- β compared to cells expressing only TCR_{Msln}. Primary human $CD8^+$ T cells expressing TCR_{Msln} only or TCR_{Msln} with an IFP were coincubated with NucLight Red^+ PANC-1 tumor cells at an effector:target (E:T) of (*A*) 20:1 or (*B*) 10:1. Images were acquired every 2 h (9 images/well, n = 4 wells/condition) via the IncuCyte live cell imaging platform from cocultures exposed to 10 ng/mL human TGF-β1 added every 48 h. The fraction of remaining tumor area/well (normalized to the first image acquired for each individual well) was plotted as a function of time with SD indicated by vertical bars. (*C*) T cells expressing TCR_{Msln} with an IFP or TCR_{Msln} only were cocultured with tumor and TGF-β1. T cell fold expansion was determined by dividing the total number of T cells from each well at the final time point (t = 168 h) by the total number of T cells at the time of acquiring the first image (t = 0). * indicates $P < 0.05$.

potential to provide a functional advantage for adoptive therapy with engineered T cells.

TGF-βR/IL-2R IFP-Expressing T Cells Exhibit Enhanced Function and Transcriptomic Reprogramming during Prolonged Exposure to TGF-β and Tumor Antigen. Given the enhanced tumor control observed in the presence of TGF-β, we next evaluated the persistence, stemness, effector function, and transcriptomic landscape of IFP-expressing T cells after long-term tumor challenge. Specifically, we analyzed these parameters following 2 wk of chronic coculture with tumor cells in the presence of TGF-β1 (*Materials and Methods*). We focused on the 2β1γ construct (with TGF-βR transmembrane domains), as it was the IFP that not only converted TGF-β signaling into IL-2/STAT5 activation (Fig. 1 *C* and *E*) but appeared most efficient at downregulating endogenous TGF-β/Smad3 signaling (*SI Appendix*, Fig. S2).

After 2 wk of chronic stimulation by tumor in the presence of TGF-β1 (*Materials and Methods*), IFP-expressing T cells compared to T cells expressing only TCR_{Msln} better maintained expression of functional effector molecules (including GZMB, TNFα, IFNγ), had higher proliferation as reflected by Ki67 levels, and achieved higher absolute numbers of more functional T cells (T cells positive for Granzyme B or positive for both TNFα and IFNγ) (Fig. 4*A* and *SI Appendix*, Fig. S4), suggesting sustained activation and functionality under immunosuppressive conditions, consistent with the observed tumor control in the presence of TGF-β (Fig. 3).

To analyze the transcriptional programs associated with such functional differences in more depth, single-cell RNA sequencing (scRNA-seq) of T cells was performed at the end of the 14-d coculture with tumor in the presence of TGF-β. IFP-expressing T cells displayed enrichment in pathways associated with effector functions and survival, such as cytolytic potential and IL-2/STAT5 signaling, and downregulation of the exhaustion pathway signature (Fig. 4*B*). Notably, IFP-expressing cells exhibited elevated expression of IL7R and GNLY (Fig. 4*C*), indicative of an enhanced memory signature and cytotoxic potential, respectively. Furthermore, other key genes associated with stemness and self-renewal potential, including TCF7, LEF1, SELL, and CCR7, were also upregulated in the IFP-expressing population (Fig. 4*C*), suggesting preservation of stemness qualities and self-renewal potential, which likely contributed to the observed superior persistence and antitumor activity.

GSEA further confirmed the functional advantages conferred by the TGF-βR/IL-2R IFP. Pathways related to T cell cytotoxicity, antigen-receptor signaling, and the IL-2/STAT5 signaling pathway were significantly enriched in the IFP-expressing T cells (*SI Appendix*, Fig. S5). These findings suggest that engineering T cells with the TGF-βR/IL-2R IFP not only provides protection from TGF-β-mediated dysfunction but also promotes a more functional phenotype with stemness and effector signatures, which have been associated with sustained therapeutic efficacy in solid tumors (27, 28).

Discussion

Adoptive therapy with engineered T cells has thus far achieved limited efficacy against the broad range of solid tumors. Immunosuppressive factors in the TME such as TGF-β represent major obstacles, ultimately limiting the persistence, expansion, and effector functions of infused T cells. To address this challenge, we engineered an IFP that couples the extracellular TGF-β receptor chains (TGF-βRI and TGF-βRII) with the intracellular domains of the IL-2 receptor signaling chains (IL-2Rβ and IL-2Rγ) (12, 18), enabling tumor-infiltrating T cells to both disrupt and convert suppressive TGF-β signals into proliferative, prosurvival IL-2-like signals. Our results demonstrate that this IFP enhances T cell function when coexpressed with human tumor-specific T cell receptors (TCRs) in the setting of persistent exposure to tumor in a milieu containing TGF-β, providing a foundation for a next generation of armored T cell therapies.

Compared to alternative targeting approaches, this IFP offers unique advantages for overcoming TGF-β–mediated immunosuppression, which is a major barrier in many epithelial cancers, including pancreatic, colorectal, prostate, and breast tumors (29). TGF-β exerts multiple immunosuppressive effects by dampening T cell effector function, promoting regulatory T cell (Treg) expansion, and contributing to a fibrotic and exclusionary TME (30–32). Previous strategies to mitigate this pathway have included systemic TGF-β blockade or interfering with downstream signaling from the TGF-βR by T cell expression of a dominant-negative TGF-βRII (dnTGF-βRII) (22, 33). Both of these strategies have clear limitations, as a dnTGF-βRII can abrogate TGF-βR signaling and promote enhanced activity (10) but lacks the ability to deliver compensatory prosurvival signals essential for sustaining T cell activity, and systemic blockade of TGF-β not only also fails to deliver prosurvival signals but often results in significant toxicities, including autoimmunity, bleeding, and cardiovascular complications as a consequence of the critical roles of TGF-β in

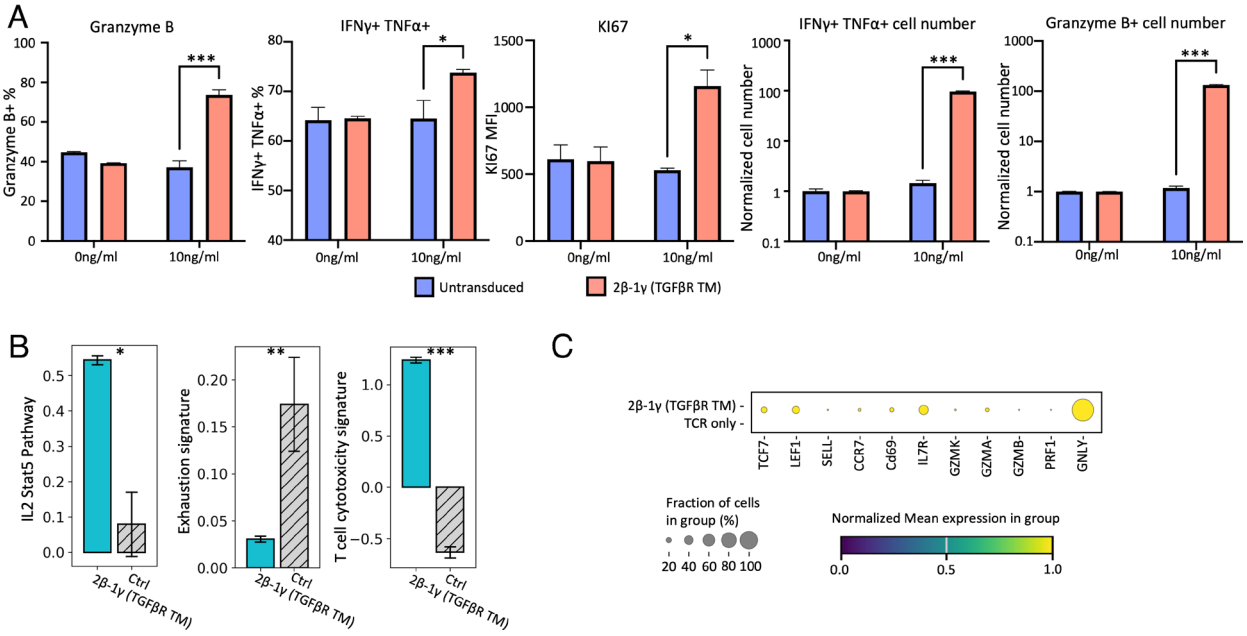

Fig. 4. T cells expressing TCR_{Msln} with a TGF-βR/IL-2R IFP (2β-1γ) following prolonged coculture with tumor cells and TGF- β1 supplementation exhibit enhanced functionality and global transcriptomic changes associated with self-renewal capacity compared to cells expressing TCR_{Msln} only. (*A* and *B*) Primary $CD8^+$ T cells expressing TCR_{Msln} only or TCR_{Msln} with an IFP were cocultured with NucLight Red^+ PANC-1 tumor cells. Every 48 h, fresh PANC-1 tumor cells in the same numbers as initially plated were added to the coculture to sustain persistent interactions with tumor cells. Exogenous TGF-β1 at 10 ng/mL was also added at coculture initiation and then every 48 h. No exogenous IL-2 was provided. At 2 wk post coculture initiation, T cells were harvested from the wells and analyzed for expression of selected proteins by flow cytometry (*A*) and selected gene expression signatures by scRNA-seq (*B*). Enhanced function was observed in IFP-expressing cells, as evidenced by increased frequencies or MFI of cells expressing the indicated proteins (*Left* three panels in *A*) and ~100 fold increase in absolute cell numbers of cells expressing those proteins (*Right* two panels in *A*). Cell counts were normalized to TCR_{Msln}-only T cells cocultured with tumor cells without TGF-β1 supplementation. * indicates $P < 0.05$, ** indicates $P < 0.01$, *** indicates $P < 0.001$. (*B*) Pathway enrichment score for pathways differentially enriched in T cells with the IFP compared to control T cells at 2 wk post coculture as in panel *A*. * indicates $P < 0.05$, ** indicates $P < 0.01$, *** indicates $P < 0.001$. (*C*) Bubble plots of expression of signature genes significantly different ($P < 0.05$) in $CD8^+$ T cells expressing TCR_{Msln} only or TCR_{Msln} with an IFP from scRNA-seq data at week 2 following chronic exposure to tumor and TGF-β1. Both color and size indicate the effect size. IFP-expressing T cells had higher levels of stemness and cytotoxic genes.

tissue homeostasis (34). In contrast, the described IFP minimizes off-target toxicity, as IFP activity is restricted to the engineered T cells and conditionally activated only in TGF-β rich microenvironments, thus largely localizing activity to the TME, which should minimize the potential for toxicity outside the TME. Moreover, by incorporating the IL-2 receptor intracellular domain, the IFP also supports proliferation and survival of the engineered tumor-reactive T cells. While several recent studies have examined TGF-β signal-converting constructs such as TGF-βR fusions with intracellular 4-1BB or cytokine receptor domains, or CAR antibody ectodomains that directly bind TGF-β (35–38), these synthetic molecules have been pursued largely in CAR-T cells, which already possess strong built-in costimulatory/survival signals. This makes it difficult to distinguish the unique contribution of costimulatory or cytokine signaling from the synthetic receptor, as any added benefit may be masked or enhanced by the robust CAR costimulatory signaling background. In contrast, our study rigorously designed and evaluated IFPs converting TGF-β signals to IL-2 signals in TCR-engineered T cells, which lack synthetic costimulatory signals and are therefore directly dependent on compensatory signals. Through cellular and molecular analyses, we unveiled that the IFP provides distinct proliferative and functional advantages in TCR-T cells targeting solid tumors with characteristically low tumor antigen density in the presence of TGF-β. By engineering and screening four structurally distinct IFPs, we identified two that effectively convert TGF-β signals into IL-2–like activation, highlighting the importance of domain compatibility and the distinct benefit of this approach in the TCR-T cell context.

This IFP also offers unique advantages compared with alternative approaches for providing T cells with IL-2 signals, which promote survival, proliferation, and cytotoxicity. High-dose IL-2 therapy was one of the earliest FDA-approved immunotherapies, with efficacy as a single agent demonstrated for treatment of metastatic melanoma and renal cell carcinoma. High-dose IL-2 is also often administered in association with cell therapies targeting other tumors (39), but clinical utility has been hampered by systemic toxicities, including capillary leak syndrome and renal and cardiovascular complications. Additionally, administered IL-2 has the propensity to expand immunosuppressive Tregs due to their natural expression of not only IL-2Rβ and IL-2Rγ but also IL-2Rα (CD25), thereby establishing the high-affinity IL-2R leading to Treg proliferation and survival and further compromising antitumor immunity (40). Moreover, the short serum half-life of IL-2 requires frequent dosing, which increases complexity and can further exacerbate side effects (40). While strategies such as constitutive expression of IL-2 in CAR-T cells have been explored, such approaches remain limited by risks of cytokine release syndrome, nonspecific expansion of bystander cells, and Treg expansion within the TME. The IFP design addresses these concerns by providing cellular and spatially restricted, TGF-β–dependent IL-2 intracellular signaling exclusively within engineered T cells, thereby mitigating risks of systemic IL-2 toxicity, avoiding the induction of Treg expansion, and preserving IL-2 signaling exclusively within the infused therapeutic T cells. Recent advances in IL-2 delivery now also include engineered IL-2 variants with reduced CD25 binding to limit Treg activation, as well as IL-2 fused to anti-CD8 antibodies for targeted delivery to $CD8^+$ T cells

(41–43). While these strategies provide means to enhance IL-2 signaling preferentially in tumor-reactive $CD8^+$ T cells, they require continued administration and the cells may still remain vulnerable to suppression mediated by TGF-β, including cell cycle arrest and inhibition of proliferation (26). By converting suppressive TGF-βR signals into IL-2R signals, the IFP offers a distinct advantage over these recent IL-2 delivery strategies.

Beyond enhancing ACT, the IFP has the potential to synergize ACT with other immunotherapies such as Immune Checkpoint Blockade (ICB). ICB has shown efficacy in several solid tumors, but the mechanisms of reinvigorating progenitor exhausted endogenous T cells via systemic inhibition of PD-1 or inducing new responses by blocking CTLA-4 differ fundamentally from that of engineered ACT, which provides de novo abundant tumor-specific effector cells. Only limited success has been achieved with ICB in solid tumors such as pancreatic cancer (44), potentially in part because the TME remains hostile due to additional inhibitory mechanisms such as via TGF-β. By enabling engineered T cells to resist TGF-β–induced inhibition while simultaneously supporting survival and persistence, this IFP may unlock new synergistic effects between ACT and ICB. Such a combination strategy represents a promising direction for future preclinical and clinical investigation.

Nonetheless, our approach is not without potential limitations. The beneficial effects of the TGF-βR/IL-2R IFP may be confined to tumors with moderate to high TGF-β expression, which is common in epithelial tumors but does not encompass all malignancies. Furthermore, intratumoral heterogeneity in TGF-β levels could result in uneven IFP activation across spatial domains. However, since TGF-β is a diffusible cytokine and often becomes globally elevated even in the serum of cancer patients (29), T cells may not need to be in close proximity to TGF-β–producing cells within the tumor to achieve effective IFP activation. Moreover, this IFP can be triggered by TGF-β concentrations as low as 0.5 ng/mL, a level commonly attained even outside the TME in the peripheral blood of patients. Evaluating IFP activity throughout the TME warrants future testing in immunocompetent murine models that recapitulate the spatial and cellular complexity of the human TME (45–47). A second potential limitation is the possibility of tonic IL-2 signaling in TGF-β–abundant contexts, which might lead to premature T cell exhaustion or apoptosis, although such exhaustion has not been observed in cells with constitutive expression of activated STAT5 (48, 49), which rather promoted durable effector states and resistance to exhaustion. A potential alternative strategy would be to design the TGF-β1R/IL-2R chain with an on/off switch (50) while still constitutively expressing the TGF-β2R/IL-2R chain, as the latter directly binds TGF-β1 and, although not capable alone of providing the IL-2R signal, can continue to function as a dominant-negative receptor. Transcriptomic profiling of IFP-engineered T cells in vivo will be essential to evaluate these alternatives and elucidate the resulting dynamics and potential obstacles.

In summary, this study establishes a rational approach to addressing two major barriers in solid tumor ACT: immunosuppression and poor expansion/persistence. By engineering a TGF-βR/IL-2R IFP that mitigates inhibitory signaling and conditionally activates prosurvival/proliferative signaling, the approach should provide a targeted, self-sustaining solution for T cells operating within hostile TMEs. This strategy may not only advance the next generation of armored engineered T cells but also provide a foundation for combinatorial immunotherapy regimens tailored to the spatial and molecular landscapes of solid tumors.

Materials and Methods

Plasmid Design and Construction. All plasmids used in this study were generated via Gibson Assembly of codon optimized gene fragments purchased from Twist Bioscience into pRRLSIN, a third-generation self-inactivating lentiviral vector. Plasmids were sequence verified using Sanger sequencing. The IFP sequences were designed by obtaining the sequences from wild type human TGF-βR and IL-2R from the NCBI (TGF-βR1: NP_004603.1, TGF-βR2: NP_001020018.1, IL-2Rβ: NP_000869.1, IL-2Rγ: NP_000197.1).

Lentivirus Production. 293T cells were cultured in RPMI 1640 media with 5% FBS (Cytiva), 5% human serum (Bloodworks Northwest), 0.6% MEM Non-Essential Amino Acids Solution (Thermo Fisher), 4 mM L-glutamine (Gibco), and 100 U/mL penicillin–streptomycin (Gibco). 293T cells were transfected at 3 million cells/10 cm dish with X-tremegene 9 transfection reagent (Millipore Sigma), according to the manufacturer's instructions, with 1.5 μg of vector DNA (either TCR only or TCR with IFP), 0.5 μg of pMD2.G (Addgene 12259), 1 μg of pMDLg/pRRE (Addgene 12251), and 1 μg of pRSV-Rev (Addgene 12253) 3rd generation lentiviral packaging and envelope plasmids. One day after transfection, media were changed. After 1 d, lentiviral supernatant was collected, filtered through a 0.45-μm PVDF filter, and concentrated 10-fold using Lenti-X Concentrator reagent (Takara Bio). The resulting lentivirus solution was stored at −80 °C.

Generation of Therapeutic T Cells with and without an IFP. PBMCs from healthy, HLA-$A2^+$ deidentified human donors were thawed and recovered after overnight culture in X-vivo 15 media with L-glutamine (Lonza) with 5% CTS Immune Cell Serum Replacement (Thermo Fisher) without cytokines. $CD4^-$ $CD62L^+$ cells were then isolated by magnetic separation with CliniMACS CD4 and CD62L selection beads (Miltenyi) on LS columns (Miltenyi) and incubated for 24 h with TransAct anti-human CD3/CD28 reagent (Miltenyi), IL-2 (100 IU/mL; Prometheus; obtained via University of Washington Pharmacy, DOH license #DRRS.FX.60550751), IL-7 (5 ng/mL; Peprotech), IL-15 (5 ng/mL; Peprotech), and IL-21 (10 ng/mL; Peprotech) at 2 million cells/mL. After this activation step, media was changed to maintain the same concentration of IL-2/7/15 and to remove IL-21, protamine sulfate added (10 μg/mL; Sigma Aldrich) and cells transduced with lentivirus generated from the TCR only construct or the constructs containing both TCR and IFP. 24 h after transduction, cells were transferred from regular culture vessels to G-Rex gas-permeable 24-well culture vessels (Wilson Wolf). To continue growth, cytokine and drug replenishment was performed every 2 to 3 d. 5 d after transduction, cells were stained with APC-conjugated tetramer for TCR_{Msln}, CD8:BV421 (Biolegend), and propidium iodide, and sorted for live $Tetramer^+$ $CD8^+$ cells. These cells, at 500,000 sorted cells per condition, were entered into a rapid expansion protocol in G-Rex 24-well vessels that contained 5 ng/mL OKT3 (Thermo Fisher) and initially doubled concentrations of IL-2, IL-7, and IL-15. At subsequent time points, medium, cytokine, and drug changes (including continued IL-2/7/15 were added at the same concentrations as before rapid expansion) every 2 to 3 d for 1 wk. At the end of this expansion period, cells were counted and used to begin coculture with tumor cells or biobanked.

In Vitro Tumor Coculture with and without TGF-β1. HLA-$A2^+$ Panc-1 pancreatic adenocarcinoma cells transduced with Nuclight Red nuclear fluorescent protein (Sartorius) were plated 1 d before beginning coculture to allow for full adherence to the tissue culture vessel. To begin coculture, $CD8^+$ TCR_{Msln}-T cells from the end of the ex vivo cell generation process were plated on top of adherent Panc-1 pancreatic adenocarcinoma cells at a fixed ratio of T cells to tumor cells. Every 48 h, Panc-1 tumor cells were added to the coculture in the same numbers as initially plated to maintain persistent interactions with tumor antigen. Exogenous TGF-β1 at 0, 1, 10, or 25 ng/mL was added throughout the cocultures starting at initiation and then every 2 d. IL-2 was also added as noted in some of the coculture conditions. Every 7 d after the start of the coculture, wells were gently rinsed for collection of the T cells from each coculture well while allowing the adherent Panc-1 cells to remain in each well. The resulting T cells were counted, and returned to a coculture with newly plated, adherent Panc-1 cells at the initial T cell:tumor cell ratio. The remaining viable T cells were biobanked. At each harvest timepoint, remaining T cells that were not needed for continuing coculture were biobanked.

For the experiments in Fig. 3 and *SI Appendix*, Figs. S3 and S4, we performed cocultures simultaneously in 96-well plates with 5,000 tumor cells per well at

effector:target (E:T) ratios of A) 20:1 or B) 10:1. Exogenous TGF-β1 and/or IL-2 was added throughout the coculture period beginning at initiation and then every 2 d. Images were acquired every 2 h (9 images/well, n = 4 wells/condition) via the IncuCyte live cell imaging platform and cell numbers at 168 h of coculture were counted.

For the experiments in Fig. 4, cocultures were established simultaneously in six-well plates with 80,000 tumor cells per well at effector:target (E:T) ratios of 10:1. Every 2 d, fresh Panc-1 tumor cells were added to the coculture in the same numbers as initially plated to maintain persistent interactions with tumor cells. Exogenous TGF-β1 at 0, 1, 10, or 25 ng/mL was added at initiation of the cocultures and then every 2 d. No exogenous IL-2 was provided throughout the coculture. At day 7, nonadherent T cells were gently collected by rinsing each well, leaving the adherent Panc-1 cells undisturbed. T cells were counted, and the appropriate number of cells needed to maintain a 10:1 T cell-to-tumor cell ratio was transferred onto freshly plated Panc-1 cells to initiate a new round of coculture. T cells were harvested on day 14 for downstream analyses by flow cytometry and scRNA-seq. T cell numbers for IFNγ$^+$ TNFα$^+$ or Granzyme B$^+$ T cells were calculated by multiplying the total number of recovered T cells by the frequency of each subset as measured by flow cytometry, and normalizing to the initial input cell number. When only a fraction of T cells was used during weekly population reset, total expansion was extrapolated based on the proportion of cells transferred.

IncuCyte Assay. The IncuCyte NucLight Red Lentivirus Reagent (Essen Biosciences, 4625) was used to transduce Panc-1 cells according to the company's standard infection protocol. Transduced cells were purified and purity confirmed on a BD FACS Aria II flow cytometry instrument. For Panc-1 coculture experiments, 5,000 tumor cells were plated in 96-well plates and allowed to adhere overnight. T cells were added the following day at a 20:1 or 10:1 T cell to tumor cell ratio. Exogenous TGF-β1 or IL-2 were supplemented every 48 h. Tumor cell killing was monitored in the IncuCyte ZOOM or S3 and quantified by the loss of red signal (Total Red Object Integrated Intensity [red calibrated unit/micrometer/image]). At 7 d after the start of the coculture, we gently rinsed and collected T cells from each coculture well, allowing the adherent Panc-1 cells to stay in each well. The resulting T cells were counted, diluted to a volume required for a 10:1 T cell:tumor cell ratio, and returned to coculture wells with newly plated, adherent Panc1 cells. We repeated the coculture and rechallenge processes several times until the final harvest time point. For Fig. 3*C* and *SI Appendix*, Fig. S3*C*, T cell fold-expansion was determined by dividing the total number of T cells quantified from each well at the final time point (t = 168 h) divided by the total number of T cells at the time the first image was acquired (t = 0).

Flow Cytometry of T Cells. For analysis of phospho-Stat5 and phospho-Smad3, primary CD8 T cells were washed twice with X-VIVO media to remove serum and rested overnight in the absence of serum (200,000 cells/well in 12-well plates with 2 mL of X-VIVO media). Cells were stimulated with the indicated amounts of recombinant TGF-β or IL-2 for 15 min at 37 °C, followed by fixation/permeabilization and staining with a phospho-specific (Y694) STAT5 antibody (clone 47, BD Biosciences 612599) or with a phospho-specific SMAD2 (S465/S467)/SMAD3 (S423/S425) antibody (clone O72-670, BD Biosciences 562586).

For p-STAT5 staining, cells were fixed by adding 18.75% v/v 16% PFA directly to the stimulation media and incubating at room temperature for 10 min. Cells were then centrifuged at 1,350 rpm for 4 min to remove media and washed once with FACS buffer. Cells were permeabilized by slowly resuspending cell pellets in 50 μL/well ice-cold Phosflow Perm Buffer III (BD Biosciences, 558050) and incubated on ice for 20 min. Cells were washed twice in FACS buffer before staining with p-STAT5 antibody resuspended in FACS buffer 1:30 at 4 °C for 45 min.

For pSMAD2/pSMAD3 staining, cells were fixed and permeabilized using 50 μL/well Cytofix/Cytoperm buffer (BD Biosciences, 554714) for 20 min at room temperature. Cells were then washed with 100 μL/well perm/wash buffer and stained with pSMAD2/pSMAD3 antibody resuspended in perm/wash buffer 1:50 at 4 °C for 45 min. Cells were then washed with FACS buffer and resuspended in FACS buffer for analysis via flow cytometry.

For phenotypic analysis, T cells were harvested at the end of chronic tumor coculture stimulation and stained for surface markers with anti-CD8:BUV395 (Biolegend) antibodies. Cells were fixed and permeabilized using the eBioScience Foxp3/Transcription Factor Staining Buffer Set (Thermo Fisher). Afterward, intracellular/intranuclear targets were labeled with anti-Ki67:PE-Cy7 (BD) antibodies.

To test for cell polyfunctionality, the harvested cells were restimulated by incubation with eBioscience Cell Stimulation Cocktail at 1× concentration (Thermo Fisher) for 3 to 4 h at 37 °C. Afterward, the cells were stained with Fixable Aqua Dead Cell Stain Kit (Thermo Fisher), and then for surface markers using anti-CD8:PerCP-Cy5.5 antibody (Biolegend). Following cell surface staining, the cells were fixed and permeabilized cells using the BD CytoFix/CytoPerm Fixation/Permeabilization Kit (BD Biosciences), and then stained for intracellular markers using IFNγ:APC, TNFα:BV786, and Granzyme B:BV421 antibodies (Biolegend).

To test for cell proliferation in response to stimulation, primary human CD8$^+$ T cells were activated overnight with anti-CD3/CD28 Dynabeads on day 0 and transduced with control or IFP constructs on day 1. After 4 d of continued culture in presence of IL-2, IL-7, IL-15 to allow for transgene expression (transduction marker NGFR alone for control, NGFR + IFP for the IFP condition), cells were washed and labeled with CTV (Thermo Fisher) for 20 min in the dark at room temperature and stimulated with recombinant human TGF-β1 or IL-2 at the indicated concentrations every 48 h. After 5 d, transgene expressing (NGFR$^+$) cell proliferation (as reflected by dilution of CTV label via flow cytometry) was measured by quantifying CTV signal per cell.

Bulk and Single-Cell RNA-seq. For bulk RNA-seq, T cells were activated on Day 0, transduced on Day 1, and cultured with TGF-β for 10 d. Cells were then sorted on Day 10 for live, transduction marker–positive populations. The cells were spun into cell pellets, snap-frozen, and stored at −80 °C. From these cell pellets, RNA for bulk RNA-seq was extracted using the AllPrep Micro-DNA/RNA extraction kit (Qiagen). The resulting RNA samples were sequenced using low-input bulk RNA-seq workflows by BGI.

For single cell RNA-seq, T cells were harvested at day 14 of chronic tumor coculture with 10 ng/mL TGF-β1 supplemented throughout the coculture initially for staining with CD8:BV421 (Biolegend) and propidium iodide. The cells were then sorted to obtain a live CD8$^+$ T cell population. The resulting sorted cells were processed using Chromium Next GEM Single Cell 3′ Kit v3.1 (10× Genomics), pooled together, and sequenced on an Illumina NovaSeq flow cell (paired end read; read 1 depth: 28 cycles; read 2 depth: 90 cycles) following the manufacturer's instructions.

Bulk RNA-seq Analysis. Raw read counts were extracted and then normalized by their library size factors, reads, and gene lengths, which was then used to calculate differentially expressed genes. Detailed information on trimming, alignment, and quantification are similar to what we previously reported (51–54). GSEA (55) was performed with GSEA (v4.1.0); log2 fold changes were calculated with a +1 pseudocount to account for zero-count genes and avoid infinite values.

Single-Cell RNA-seq Analysis. Single-cell RNA-seq analysis was performed as previously described (56–58). Briefly, sequence reads were demultiplexed and processed using Cellranger pipeline version 7.1.0 with alignment to the reference human genome hg38. Aligned single cell read data were further processed using custom code based around the Scanpy package (59) in Python 3. In brief, cells from each sample were combined into a concatenated object. Cells were then filtered with ≥500 genes and ≥1,000 counts, then filtered based on: 1) $<10^4$ counts per cell (library size); 2) <4,000 detected genes per cell; and 3) the proportion of mitochondrial gene counts (mitochondrial gene UMIs/total UMIs) <10%. Doublets were removed by Scrublet. After QC-based filtering, Scanpy was used to normalize cells via CPM normalization (UMI count per cell was set to 10^6) and log1p transformation (natural log of CPM plus one). Principal component analysis (PCA) was performed. Gene set enrichment was done via GSEA (v4.1.0) for rank-based metrics. Mann–Whitney *U* tests were utilized for statistics, *P*-values, unless otherwise specified in the legend or on the plot.

Statistical Analyses. All the data are shown as the means ± SEM except for Incucyte assays, which are shown as mean ± SD. Data comparisons between two samples were tested by Student's *t* test, and those among multiple samples were tested by ANOVA. The significance level was set at α = 0.05. This means that a difference was significant when the *P* value was less than 0.05. The *P* values are generally represented as follows: $^*P < 0.05$, $^{**}P < 0.01$, and $^{***}P < 0.001$. GraphPad Prism was used to generate the graphs and perform the statistical analyses.

Data, Materials, and Software Availability. All data, code, and materials used in the analysis are available for purposes of reproducing or extending the analysis. Cell lines and constructs will be shared after execution of applicable materials transfer agreements (MTAs). Processed bulk and single-cell RNA-seq data were deposited onto Mendeley data (https://data.mendeley.com/preview/hdzwy6cdmz?a=e2554239-ea65-47d4-a5a9-302a213d5cb1) (60). All other data are included in the manuscript.

ACKNOWLEDGMENTS. We greatly appreciate the help of the core facilities at Fred Hutch for performing critical experiments for this investigation. The Fred Hutch Genomics Shared Resource performed next generation sequencing workflows. The Fred Hutch Immune Monitoring Core generated Major Histocompatibility Complex class I (MHC I)-peptide tetramers for our use in flow cytometry and cell sorting. The Fred Hutch Flow Cytometry Core performed flow cytometry and cell sorting services. We thank BioRender.com for enabling the creation of schematics used in this manuscript. This study was supported in part by research grants from the Fred Hutch Translational Data Science Integrated Research Center (226473-99; Y.S. and P.D.G.), NIH (CA18029 and CA225517; P.D.G.), NIH (K99CA293142; Y.S.), and Parker Institute for Cancer Immunotherapy (P.D.G.); the Damon Runyon Cancer Research Foundation Quantitative Biology Fellowship (DRQ-13-22; Y.S.), Mahan Fellowship at Herbold Computational Biology Program of Fred Hutchinson Cancer Center (Y.S.), Hartwell Innovation Award from the Hartwell Innovation Fund and Swim Across America Award (Y.S.), NIH/NCI Cancer Center Support Grant P30 CA015704 (Y.S. and P.D.G.), and NIH grants S10-OD-020069 and S10-OD-028685 (Fred Hutch Scientific Computing). This research was also supported by the Genomics & Bioinformatics Shared Resource (RRID:SCR_022606) and Flow Cytometry Shared Resource (RRID:SCR_022613) of the Fred Hutch/University of Washington/Seattle Children's Cancer Consortium (P30 CA015704). P.D.G. is on the Scientific Advisory Board of Affini-T Therapeutics, Elpiscience, Immunoscape, Earli, Rapt, Catalio, and Nextech, was a scientific founder of Affini-T and Juno Therapeutics, and has received research support from Affini-T and Lonza.

Author affiliations: [a]Program in Immunology, Translational Science and Therapeutics Division, Fred Hutchinson Cancer Center, Seattle, WA 98109; [b]Herbold Computational Biology Program, Vaccine and Infectious Disease Division, Fred Hutchinson Cancer Center, Seattle, WA 98109; [c]Department of Cellular Genetics, Wellcome Genome Campus, Wellcome Sanger Institute, Hinxton CB10 1SA, United Kingdom; [d]Cambridge Stem Cell Institute, Cambridge Biomedical Campus, University of Cambridge, Cambridge CB2 0AW, United Kingdom; [e]Division of Clinical Research and Innovation, Biomedical Data Science Centre, Lausanne University Hospital and University of Lausanne, Lausanne CH-1005, Switzerland; [f]Department of Immunology, University of Washington, Seattle, WA 98109; and [g]Department of Medicine/Oncology, University of Washington, Seattle, WA 98109

Author contributions: Y.S., A.T., and P.D.G. designed research; Y.S., A.T., L.V.W., C.M.J., S.R.M., and D.G.C. performed research; Y.S., A.T., L.V.W., C.M.J., S.R.M., D.G.C., R.G., and P.D.G. analyzed data; and Y.S., A.T., and P.D.G. wrote the paper.

1. A. G. Chapuis *et al.*, T cell receptor gene therapy targeting WT1 prevents acute myeloid leukemia relapse post-transplant. *Nat. Med.* **25**, 1064–1072 (2019).
2. K. G. Anderson, I. M. Stromnes, P. D. Greenberg, Obstacles posed by the tumor microenvironment to T cell Activity: A case for synergistic therapies. *Cancer Cell* **31**, 311–325 (2017).
3. M. Spiga *et al.*, Harnessing the tumor microenvironment to boost adoptive T cell therapy with engineered lymphocytes for solid tumors. *Semin. Immunopathol.* **46**, 8 (2024).
4. L. E. Cheng, C. Ohlén, B. H. Nelson, P. D. Greenberg, Enhanced signaling through the IL-2 receptor in CD8+ T cells regulated by antigen recognition results in preferential proliferation and expansion of responding CD8+ T cells rather than promotion of cell death. *Proc. Natl. Acad. Sci. U.S.A.* **99**, 3001–3006 (2002).
5. A. Taber, A. Konecny, S. K. Oda, J. Scott-Browne, M. Prlic, TGF-β broadly modifies rather than specifically suppresses reactivated memory CD8 T cells in a dose-dependent manner. *Proc. Natl. Acad. Sci. U.S.A.* **120**, e2313228120 (2023).
6. M. Ahmadzadeh, S. A. Rosenberg, TGF-β1 attenuates the acquisition and expression of effector function by tumor antigen-specific human memory CD8 T cells. *J. Immunol.* **174**, 5215–5223 (2005).
7. R. J. Kovacs *et al.*, Cardiac safety of TGF-β receptor I kinase inhibitor LY2157299 monohydrate in cancer patients in a first-in-human dose study. *Cardiovasc. Toxicol.* **15**, 309–323 (2015).
8. J. Massagué, D. Sheppard, TGF-β signaling in health and disease. *Cell* **186**, 4007–4037 (2023).
9. J. P. Siegel, R. K. Puri, Interleukin-2 toxicity. *J. Clin. Oncol.* **9**, 694–704 (1991).
10. V. Narayan *et al.*, PSMA-targeting TGFβ-insensitive armored CAR T cells in metastatic castration-resistant prostate cancer: A phase 1 trial. *Nat. Med.* **28**, 724–734 (2022).
11. S. A. Rosenberg *et al.*, Durable complete responses in heavily pretreated patients with metastatic melanoma using T-cell transfer immunotherapy. *Clin. Cancer Res.* **17**, 4550–4557 (2011).
12. B. H. Nelson, J. D. Lord, P. D. Greenberg, Cytoplasmic domains of the interleukin-2 receptor β and γ chains mediate the signal for T-cell proliferation. *Nature* **369**, 333–336 (1994).
13. S. K. Oda *et al.*, A Fas-4-1BB fusion protein converts a death to a pro-survival signal and enhances T cell therapy. *J. Exp. Med.* **217**, e20191166 (2020).
14. S. K. Oda *et al.*, A CD200R-CD28 fusion protein appropriates an inhibitory signal to enhance T-cell function and therapy of murine leukemia. *Blood* **130**, 2410–2419 (2017).
15. M. E. Prosser, C. E. Brown, A. F. Shami, S. J. Forman, M. C. Jensen, Tumor PD-L1 co-stimulates primary human CD8(+) cytotoxic T cells modified to express a PD1:CD28 chimeric receptor. *Mol. Immunol.* **51**, 263–272 (2012).
16. A. P. Hinck, Structural studies of the TGF-βs and their receptors–Insights into evolution of the TGF-β superfamily. *FEBS Lett.* **586**, 1860–1870 (2012).
17. X. Wang, M. Rickert, K. C. Garcia, Structure of the quaternary complex of interleukin-2 with its alpha, beta, and gammac receptors. *Science* **310**, 1159–1163 (2005).
18. Y. Nakamura *et al.*, Heterodimerization of the IL-2 receptor beta- and gamma-chain cytoplasmic domains is required for signalling. *Nature* **369**, 330–333 (1994).
19. S. Radaev *et al.*, Ternary complex of transforming growth factor-beta1 reveals isoform-specific ligand recognition and receptor recruitment in the superfamily. *J. Biol. Chem.* **285**, 14806–14814 (2010).
20. S. H. Ross, D. A. Cantrell, Signaling and function of interleukin-2 in T lymphocytes. *Annu. Rev. Immunol.* **36**, 411–433 (2018).
21. J. Liang *et al.*, The phosphorylation of the Smad2/3 linker region by nemo-like kinase regulates TGF-β signaling. *J. Biol. Chem.* **296**, 100512 (2021).
22. C. C. Kloss *et al.*, Dominant-negative TGF-β receptor enhances PSMA-Targeted human CAR T cell proliferation and augments prostate cancer eradication. *Mol. Ther.* **26**, 1855–1866 (2018).
23. L. Das, A. D. Levine, TGF-beta inhibits IL-2 production and promotes cell cycle arrest in TCR-activated effector/memory T cells in the presence of sustained TCR signal transduction. *J. Immunol.* **180**, 1490–1498 (2008).
24. S. Ahmed, A.-D. Bradshaw, S. Gera, M. Z. Dewan, R. Xu, The TGF-β/Smad4 signaling pathway in pancreatic carcinogenesis and its clinical significance. *J. Clin. Med.* **6**, 5 (2017).
25. K. S. Shim, K. H. Kim, W. S. Han, E. B. Park, Elevated serum levels of transforming growth factor-β1 in patients with colorectal carcinoma. *Cancer* **85**, 554–561 (1999).
26. J. D. Campbell *et al.*, Suppression of IL-2-induced T cell proliferation and phosphorylation of STAT3 and STAT5 by tumor-derived TGF beta is reversed by IL-15. *J. Immunol.* **167**, 553–561 (2001).
27. L. Gattinoni *et al.*, A human memory T cell subset with stem cell-like properties. *Nat. Med.* **17**, 1290–1297 (2011).
28. A. D. Waldman, J. M. Fritz, M. J. Lenardo, A guide to cancer immunotherapy: From T cell basic science to clinical practice. *Nat. Rev. Immunol.* **20**, 651–668 (2020).
29. S. Liu, J. Ren, P. ten Dijke, Targeting TGFβ signal transduction for cancer therapy. *Signal Transduct. Target. Ther.* **6**, 8 (2021).
30. K. K. Kim, D. Sheppard, H. A. Chapman, TGF-β1 signaling and tissue fibrosis. *Cold Spring Harb. Perspect. Biol.* **10**, a022293 (2018).
31. J. M. Moreau, M. Velegraki, C. Bolyard, M. D. Rosenblum, Z. Li, Transforming growth factor-β1 in regulatory T cell biology. *Sci. Immunol.* **7**, eabi4613 (2022).
32. W. J. Chen, TGF-β regulation of T cells. *Annu. Rev. Immunol.* **41**, 483–512 (2023).
33. H. Ungefroren, Blockade of TGF-β signaling: A potential target for cancer immunotherapy? *Expert Opin. Ther. Targets* **23**, 679–693 (2019).
34. Z. Deng *et al.*, TGF-β signaling in health, disease and therapeutics. *Signal Transduct. Target. Ther.* **9**, 61 (2024).
35. Z. L. Chang *et al.*, Rewiring T-cell responses to soluble factors with chimeric antigen receptors. *Nat. Chem. Biol.* **14**, 317–324 (2018).
36. T. Matikhina, C. J. Cohen, Targeting TGFβ with chimeric switch receptor and secreted trap to improve T cells anti-tumor activity. *Front. Immunol.* **15**, 1460266 (2024).
37. S. Zheng, X. Che, K. Zhang, Y. Bai, H. Deng, Potentiating CAR-T cell function in the immunosuppressive tumor microenvironment by inverting the TGF-β signal. *Mol. Ther.* **33**, 688–702 (2025).
38. C. Beck *et al.*, Development of a TGFβ-IL-2/15 switch receptor for use in adoptive cell therapy. *Biomedicines* **11**, 459 (2023).
39. S. A. Rosenberg *et al.*, Use of tumor-infiltrating lymphocytes and interleukin-2 in the immunotherapy of patients with metastatic melanoma. *N. Engl. J. Med.* **319**, 1676–1680 (1988).
40. R. N. Schwartz, L. Stover, J. P. Dutcher, Managing toxicities of high-dose interleukin-2. *Oncology (Williston Park)* **16**, 11–20 (2002).
41. R. Dehghan *et al.*, Efficacy and antitumor activity of a mutant type of interleukin 2. *Sci. Rep.* **12**, 5376 (2022).
42. Z. Sun *et al.*, A next-generation tumor-targeting IL-2 preferentially promotes tumor-infiltrating CD8+ T-cell response and effective tumor control. *Nat. Commun.* **10**, 3874 (2019).
43. P. Kaptein *et al.*, CD8-targeted IL2 unleashes tumor-specific immunity in human cancer tissue by reviving the dysfunctional T-cell pool. *Cancer Discov.* **14**, 1226–1251 (2024).
44. I. M. Stromnes *et al.*, Insufficiency of compound immune checkpoint blockade to overcome engineered T cell exhaustion in pancreatic cancer. *J. Immunother. Cancer* **10**, e003525 (2022).
45. I. M. Stromnes *et al.*, T cells engineered against a native antigen can surmount immunologic and physical barriers to treat pancreatic ductal adenocarcinoma. *Cancer Cell* **28**, 638–652 (2015).
46. K. G. Anderson *et al.*, Engineered adoptive T-cell therapy prolongs survival in a preclinical model of advanced-stage ovarian cancer. *Cancer Immunol. Res.* **7**, 1412–1425 (2019).
47. S. Srivastava *et al.*, Immunogenic chemotherapy enhances recruitment of CAR-T cells to lung tumors and improves antitumor efficacy when combined with checkpoint blockade. *Cancer Cell* **39**, 193–208.e10 (2021).
48. T. W. Hand *et al.*, Differential effects of STAT5 and PI3K/AKT signaling on effector and memory CD8 T-cell survival. *Proc. Natl. Acad. Sci. U.S.A.* **107**, 16601–16606 (2010).
49. J.-C. Beltra *et al.*, Stat5 opposes the transcription factor Tox and rewires exhausted CD8+ T cells toward durable effector-like states during chronic antigen exposure. *Immunity* **56**, 2699–718.e11 (2023).
50. M. Jan *et al.*, Reversible on- and off-switch chimeric antigen receptors controlled by lenalidomide. *Sci. Transl. Med.* **13**, eabb6295 (2021).
51. Y. Su *et al.*, Single-cell analysis resolves the cell state transition and signaling dynamics associated with melanoma drug-induced resistance. *Proc. Natl. Acad. Sci. U.S.A.* **114**, 13679–13684 (2017).
52. Y. Su *et al.*, Phenotypic heterogeneity and evolution of melanoma cells associated with targeted therapy resistance. *PLoS Comput. Biol.* **15**, e1007034 (2019).

53. Y. Su *et al.*, Multi-omic single-cell snapshots reveal multiple independent trajectories to drug tolerance in a melanoma cell line. *Nat. Commun.* **11**, 2345 (2020).
54. J. Du *et al.*, Raman-guided subcellular pharmaco-metabolomics for metastatic melanoma cells. *Nat. Commun.* **11**, 4830 (2020).
55. A. Subramanian *et al.*, Gene set enrichment analysis: A knowledge-based approach for interpreting genome-wide expression profiles. *Proc. Natl. Acad. Sci. U.S.A.* **102**, 15545–15550 (2005).
56. Y. Su *et al.*, Multi-omics resolves a sharp disease-state shift between mild and moderate COVID-19. *Cell* **183**, 1479–1495.e20 (2020).
57. J. W. Lee *et al.*, Integrated analysis of plasma and single immune cells uncovers metabolic changes in individuals with COVID-19. *Nat. Biotechnol.* **40**, 110–120 (2022).
58. Y. Su *et al.*, Multiple early factors anticipate post-acute COVID-19 sequelae. *Cell* **185**, 881–95.e20 (2022).
59. F. A. Wolf, P. Angerer, F. J. Theis, Scanpy: Large-scale single-cell gene expression data analysis. *Genome Biol.* **19**, 15 (2018).
60. Y. Su *et al.*, Data from "A TGF-βR/IL-2R immunomodulatory fusion protein transforms immunosuppression into T cell activation to enhance adoptive T cell therapy." Mendeley Data. https://dx.doi.org/10.17632/hdzwy6cdmz.1. Deposited 2 September 2025.